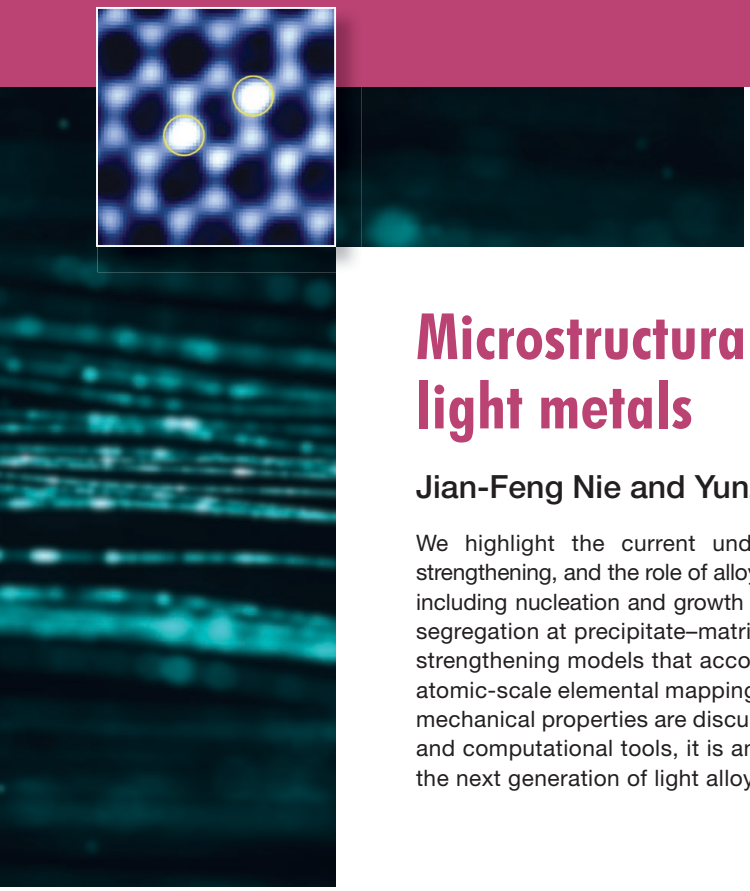


Microstructural design for advanced light metals

Jian-Feng Nie and Yunzhi Wang

We highlight the current understanding of mechanisms of phase transformation, strengthening, and the role of alloying elements in aluminum, magnesium, and titanium alloys, including nucleation and growth of precipitates, precipitate–dislocation interactions, solute segregation at precipitate–matrix interfaces and planar defects, and the development of strengthening models that account for the real particle shape. Future directions such as atomic-scale elemental mapping and computation, and the influence of particle shape on mechanical properties are discussed. With the combination of advanced characterization and computational tools, it is anticipated that much less time will be needed to develop the next generation of light alloys.

Introduction

Advanced lightweight alloys for structural applications share a common feature—they are all strengthened by second-phase particles. The crystal structure (i.e., ordered intermetallic or solid-solution phases), volume fraction, size and shape, orientation relationship with the matrix phase and habit plane inclination, coherency state and spatial distribution of these second-phase particles, collectively called precipitate microstructure, determine the deformation behavior and mechanical properties of these alloys. While the crystal structure and volume fraction are controlled mainly by alloy composition (i.e., phase equilibria), the remaining microstructural attributes depend on specific solid-state phase transformation pathways (TPs) leading to the precipitation of these second-phase particles during a specific thermal or thermomechanical treatment. Thus, the major strategy in advanced lightweight alloy design has been to control the specific TPs for a given alloy to optimize the previously mentioned microstructure attributes, regulate microstructure–dislocation interactions and tailor the microstructure–property relationship.[1]

This article is an overview of the current understanding of mechanisms of phase transformation, strengthening, and the role of microalloying elements in Al, Mg, and Ti alloys. Emphasis is on nucleation and growth of precipitates, precipitate–dislocation interactions, solute segregation at precipitate–matrix interfaces and planar defects, and the development of strengthening models that account for the real (as opposed to an assumed spherical) particle shape in light alloys. We will show that emerging modeling and advanced characterization tools are not only adding a new understanding, but opening up new pathways for alloy design.

Aluminum alloys

Roles of microalloying elements

The key strengthening precipitate phase in binary Al-Cu alloys is θ′, which forms as a $\{001\}_\alpha$ plate, with $(001)_{\theta'}//\{001\}_\alpha$ as its broad surface. The $(001)_\theta//\{001\}_\alpha$ interface was traditionally thought to have a mixture of Cu and Al, but recent Z-contrast scanning transmission electron microscopy (STEM) imaging[2] indicated that it actually contains 100% Cu. First-principles density functional theory (DFT) calculations revealed that the presence of excessive Cu (i.e., Cu segregation) in this interface reduced the interfacial energy.[2]

Additions of 0.3 wt% Mg and 0.4 wt% Ag to Al-4 wt% Cu alloy fully replace θ′ by the Ω phase that forms as thin plates on $\{111\}_\alpha$ with an aspect ratio larger than θ′. The resultant Al-Cu-Mg-Ag alloys exhibit a tensile yield strength above 500 MPa. While it is known that Mg or Ag alone cannot facilitate Ω precipitation, their precise roles in Ω nucleation and growth are not fully understood. Atom probe tomography and Z-contrast STEM indicated that Ω evolved from preexisting Mg-Ag clusters that formed in the very early stage of

Jian-Feng Nie, Department of Materials Science and Engineering, Monash University, Australia; jianfeng.nie@monash.edu
Yunzhi Wang, Department of Materials Science and Engineering, The Ohio State University, USA; wang.363@osu.edu
doi:10.1557/mrs.2019.73

© 2019 Materials Research Society

https://doi.org/10.1557/mrs.2019.73 Published online by Cambridge University Press

decomposition, and that the Mg and Ag atoms segregated to the broad Ω/α–Al interface during Ω growth.[3–5] Recent observations using aberration-corrected Z-contrast STEM revealed that the Ag atoms segregated into a single layer adjacent to the α-Al matrix, where the Ag atoms had a graphene-like hexagonal arrangement.[5] While Mg atoms were proposed to be at the center of individual hexagons, there is no experimental evidence supporting this notion. If segregation of Ag and Mg were to reduce the interfacial energy of the interface, it would then facilitate Ω nucleation and increase the Ω aspect ratio. The enlarged aspect ratio of the Ω plates could reduce effective interparticle spacing and enhance the alloy yield strength.

In Al-Cu-Li alloys, the predominant strengthening precipitate phase is T_1 that forms as ultrathin plates on $\{111\}_\alpha$. T_1 has a much larger aspect ratio than Ω. Although T_1 is fully coherent with the α-Al matrix, its nucleation is difficult in Al-Cu-Li ternary alloys. Consequently, 0.3 wt% Mg and 0.4 wt% Ag are added to facilitate T_1 nucleation. The resultant Al-Cu-Li-Mg-Ag alloys exhibit an ultrahigh tensile yield strength exceeding 700 MPa, which makes them competitive with high-strength low-alloy steels on the basis of strength alone. Again, the precise roles of Mg and Ag in T_1 precipitation are speculative.

Studies using atom probe tomography[6,7] revealed the formation of pre-precipitate clusters of Mg atoms during early stages of aging, and the segregation of Mg and Ag to the T_1 broad face at later stages of aging. But it is unclear how the Mg-Ag co-clusters assist T_1 nucleation. Recent work on aberration-corrected Z-contrast STEM[8,9] suggested that Ag atoms segregated into a single layer that is adjacent to the α-Al matrix phase, similar to that observed in the Ω/α–Al interface. Once again, the distribution of Mg atoms in the interface is unknown due to the limitation of the Z-contrast STEM imaging technique. In the future, it will be necessary to employ atomic-resolution spectroscopy mapping techniques such as energy-dispersive x-ray spectroscopy (EDS) STEM to accurately locate Ag and Mg atoms in the precipitate–matrix interface.

Microstructure design for higher strength

Design of Al alloys for higher strength requires an improved understanding of precipitate–dislocation interactions. Existing strengthening models often assume a spherical shape for precipitates, and this assumption inevitably under- or overestimates the strengthening effect of plate-shaped particles. The traditional approach of alloy design emphasizes higher nucleation rates for a denser distribution of the precipitate. An alternative approach is to increase the plate aspect ratio (A). Assuming that the volume of each particle remains unchanged during shape change, phase-field simulated distributions of precipitates are shown in **Figure 1**a–c. With an increase in A, the number density per unit area increases, and critical resolved shear stress (ΔCRSS) increases. When A changes from 1:1 to 20:1 or 40:1, the ΔCRSS value increases from 40 MPa to 95 or 170 MPa, respectively.[10]

For θ′, Ω or T_1 plates, coherency strain exists in the direction normal to the broad surface. This strain interacts with the stress field of a dislocation when it approaches the plate (Figure 1d), and it may affect ΔCRSS. However, a recent phase-field simulation indicated that the coherency strain contributes little to strengthening.[10] The trivial effect of coherency strain on ΔCRSS is illustrated in Figure 1e–f. The dislocation configurations, with and without the consideration of coherency strain, are almost the same, after a dislocation has passed through the entire precipitate forest. The ΔCRSS values change from 77 MPa to only 80 MPa when coherency strain is considered.[10]

Many particle-strengthening models[11] assume that the maximum strength achieved during isothermal aging corresponds to a critical particle size, above which a transition from dislocation shearing to looping occurs. For precipitate plates, the critical dimension was assumed to correspond to the plate thickness, which essentially ignored the particle shape effect on strengthening. It has been reported[12] that there unlikely exists a simple critical thickness for precipitate plates. For example, T_1 plates are sheared in both peak-aged and overaged conditions after tensile fracture of Al-Cu-Li 2090 alloy.[13]

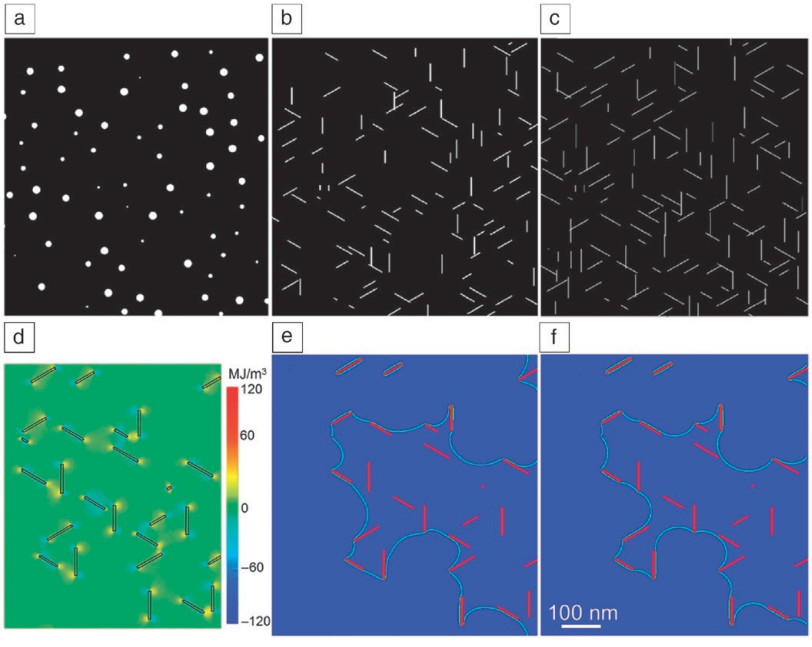


Figure 1. Phase-field-simulated distributions of θ′ precipitates with an aspect ratio of (a) 1:1, (b) 20:1, and (c) 40:1. The volume fraction and number density per unit volume of θ′ are the same in the simulations. (d) Interaction energy of stress fields of θ′ (black frame) and gliding dislocation. (e, f) Dislocation configurations with (e) and without (f) the influence of coherency strain of θ′ (A = 15:1).[10] The scale is the same in (e) and (f).

https://doi.org/10.1557/mrs.2019.73 Published online by Cambridge University Press

In the case of Al-Cu-Sn alloys that are strengthened exclusively by θ′, the Orowan equation that was modified in consideration of precipitate shape, accounts well for the age-hardening curve, with the maximum hardness corresponding to the minimum effective interprecipitate spacing.[14] This agreement between calculations and experimental data demonstrates that it is unnecessary to invoke a transition from precipitate shearing to Orowan looping to model the form of the hardness curve as a function of aging.

Since most precipitation-hardened Al alloys are multiphase, there are invariably two or more precipitate phases contributing to the maximum strength. The contribution of precipitates to the alloy yield strength is traditionally defined by simple addition of the individual contributions of the relevant phases,[11] but there is some evidence[12] that it is the mean spacing between precipitates that influences the strengthening effect. Attempts to develop a predictive strengthening model for alloys containing a multiphase dispersion of precipitates are currently restricted by a lack of understanding of interactions between precipitates and dislocations and appropriate versions of particle strengthening equations that take into account the geometry of a mixed distribution of precipitate morphologies.

Magnesium alloys

Solute clusters and heterogeneous nucleation

A technologically important group of Mg alloys are those based on the Mg–rare-earth (RE) system. These alloys exhibit an excellent age-hardening response and creep resistance. Precipitation in these alloys always involves formation of intermediate metastable phases such as β_1. While the crystal structures, morphologies, and orientations of these phases are now relatively well understood, solute clusters or aggregates formed in the early stages of precipitation are still only poorly understood. Recent observations by atomic-resolution Z-contrast STEM revealed that solute atoms tend to form short-range ordered clusters.[15] These clusters form as single- or multicolumn pillars along specific crystallographic directions (**Figure 2**a), rather than develop a cloudlike shape, which is a widely accepted notion in the literature. DFT calculations indicated that the formation of such rationally oriented, short-range ordered solute clusters is driven by the minimization of elastic strain energy associated with individual solute atoms (Figure 2b).[15]

The recognition of rationally oriented and short-range ordered solute clusters (pillars) provides an insightful clue to the mechanistic understanding of the cluster-assisted nucleation of precipitate plates. The shear displacement associated with formation of the first planar element of a precipitate platelet, such as θ′, Ω, T_1, and β_1, leads to local regions of dilation and compression in the adjacent matrix along some specific directions.[16,17] If there is an extrinsic supply of rationally oriented atomic pillars of larger solute atoms to the dilated regions, or smaller solute atoms into the compressed regions, then the strain energy associated with plate formation will be relieved, leading to an enhanced nucleation rate of the precipitate. The crystallographic orientation of such solute clusters may well determine the identity of the preferred (metastable) precipitate phase in a given trace-modified alloy.

Solute segregation

RE-free alloys based on the Mg-Sn system have received some interest for developing high-strength alloys. The age-hardening response of binary Mg-Sn alloys is weak, as the key strengthening precipitate phase β-Mg_2Sn is energetically difficult to nucleate. Ternary additions of 1 wt% Zn to Mg-Sn alloys remarkably refine β distribution and enhance the age-hardening response.[18,19] A recent study conducted by EDS-STEM mapping[20] indicated that Zn segregated strongly to the β–matrix interface, irrespective of the interfacial structure and orientation of the interface and the orientation relationship of β. The segregation layers were quite thin, and their accurate structure is unknown. Hence, it was difficult to deduce why Zn atoms segregated to the interface and whether this segregation reduced the interfacial energy to such a level that ultimately led to a significantly enhanced nucleation rate of β. Again, the use of atomic-resolution EDS-STEM may provide a vital clue to the accurate location of the segregated Zn atoms in the interface.

Mg has a hexagonal structure with fewer slip systems than Al. To readily form Mg products, the activation of twinning modes for plastic deformation is required. The control of deformation twinning during thermomechanical processes is a major technical barrier. For this reason, the nucleation,

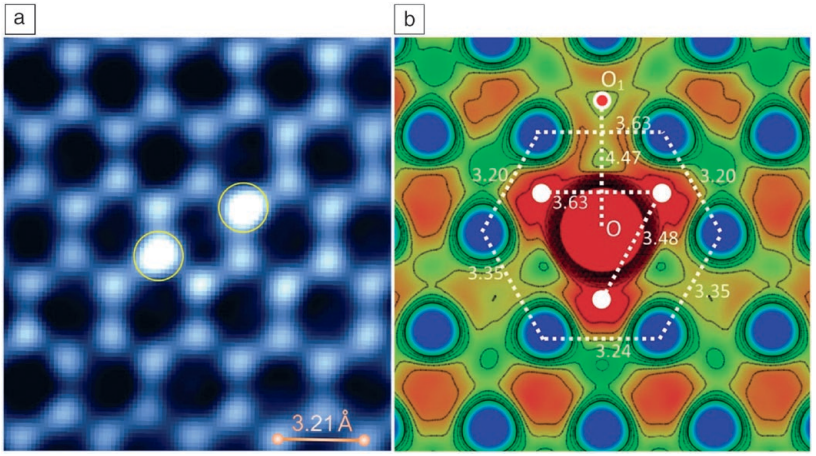


Figure 2. (a) $[0001]_\alpha$ Z-contrast scanning transmission electron microscopy image showing clusters (bright columns) of Nd atoms along $[0001]_\alpha$, (b) Charge density plot of a $(0001)_\alpha$ plane passing through a single substituted Nd atom (O position) within the Mg lattice. White discs and O_1 show key positions of Mg atoms in the (0002) layers above or below. The numbers in the plot indicate the inter-atomic bond lengths.[15]

https://doi.org/10.1557/mrs.2019.73 Published online by Cambridge University Press

growth, and transmission of deformation twins in polycrystalline alloys have been extensively studied.[21–24] Much less effort was directed to study interactions between deformation twins and solute clusters or second-phase particles. There is increasing experimental evidence demonstrating the solute segregation in coherent twin boundaries[25] (**Figure 3**a) and tilt boundaries[26] of solid-solution single-phase alloys that have been deformed and annealed (Figure 3b). Larger solutes tend to segregate to extension sites of twin boundaries or around the cores of individual dislocations in the tilt boundary, enabling the reduction of local strains in the twin or tilt boundary.

Solute segregation also occurs frequently in grain boundaries in thermomechanically processed Mg alloys.[27–31] For solutes such as Zn or Ca, segregation to grain boundaries alone (Figure 3c–d) does not effectively reduce boundary mobility.[31] However, when they co-segregate to grain boundaries, much finer recrystallized grains are obtained concomitantly. It was hypothesized that Zn and Ca co-segregate to high-energy boundaries of recrystallized grains that would otherwise grow preferentially.[31] The co-segregation may significantly reduce the boundary mobility by reducing grain-boundary energy and enhancing the solute dragging effect. A rapidly evolving understanding of segregation and co-segregation phenomena is opening up new pathways for alloy design.

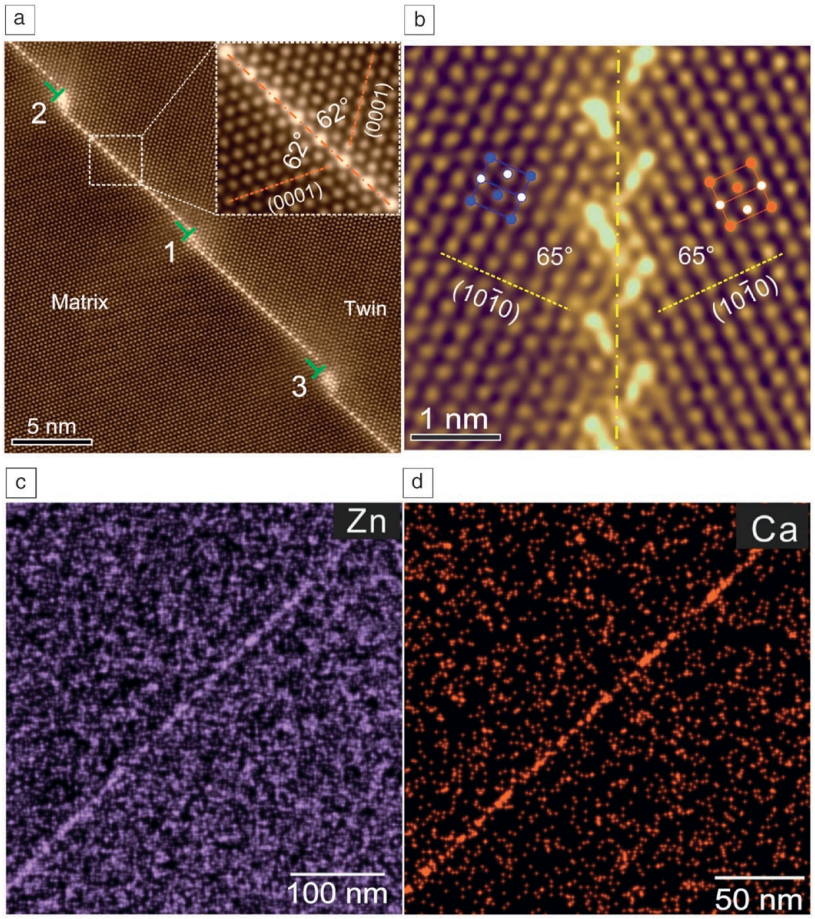


Figure 3. Atomic-scale Z-contrast scanning transmission electron microscopy images showing Gd segregation in (a) twin boundary[25] and (b) tilt boundary[26] in Mg alloys. (c, d) Energy-dispersive x-ray spectroscopy maps showing segregation of Zn or Ca to grain boundaries.[31]

Titanium alloys

Phase transformations and microstructure development

Microstructures of Ti-alloys contain primarily two phases, α precipitate (hexagonal close-packed [hcp]) and β matrix (body-centered cubic [bcc]), produced by precipitation reaction during aging treatment.[32,33] Because of symmetry-breaking associated with the bcc to hcp structural transformation following the Burgers path,[34] which involves both shear and shuffle, there are 12 crystallographically equivalent TPs, leading to 12 crystallographically equivalent structural states of α, referred to as the correspondence variants, or transformation or deformation variants.[35] In addition to the structural change, long-range atomic diffusion controls the precipitation reaction rate because of strong partitioning of different alloying elements in the α and β phases. Thus, the β → α transformation during α precipitation is a typical mix-mode (diffusional and displacive) transformation.

The Burgers path is defined in the transformation strain space and there is a significant shear component (about 10% for Ti-6Al-4V) and a volume change (about 2% for Ti-6Al-4V) associated with it. Because of this, the α precipitates have anisotropic shapes (laths or plates) with well-defined habit planes and complex defect structures at the α/β interfaces (causing growth anisotropy), with correlated spatial distributions (e.g., in the form of Widmanstätten or basket weave structures). For the same reason, the α precipitates interact strongly with preexisting stress–strain-carrying defects such as dislocations[36] and, as a consequence, any plastic deformation prior to heat treatment will work effectively in altering α precipitation and the final α + β microstructure.[37] Thus, thermomechanical processes (deformation + heat treatment) offer an additional degree of freedom to tailor the α + β microstructure for broader applications.

In addition to the previously mentioned conventional TPs (direct and defect-mediated nucleation and growth), recent studies have revealed various nonconventional TPs for α precipitation involving nucleation and growth mediated by intermediate phases (such as α′ and α″ martensites and athermal and isothermal ω phases),[38] precursory concentration modulation within the β matrix produced by

https://doi.org/10.1557/mrs.2019.73 Published online by Cambridge University Press

spinodal decomposition, pseudospinodal decomposition,[39] and spinodal decomposition of intermediate α phase obtained via congruent β → α transformation.[40] Because of these, conventional and nonconventional TPs could coexist and be intertwined during precipitation in complicated alloys such as metastable β Ti-alloys. If this is the case, the design space for microstructural engineering of Ti-alloys simply multiplies.

Effect of parent β-phase grain structure

Grain size and texture of the parent β phase have (1) direct impact on mechanical properties of the alloys and (2) profound influence on the β → α transformation (such as heterogeneous nucleation and subsequent growth at grain boundaries) and hence the final α + β microstructure.[41] Furthermore, strong texture of β grains will cause strong texture of α precipitates (called transformation texture or microtexture) through variant selection of α precipitates during precipitation by β grain boundaries[42,43] and local stress states in each β grain,[44] which is detrimental to fatigue life of Ti-alloy components.

Design of ultrafine and microtexture-free precipitate microstructures

The complicated TPs in Ti-alloys and the complexity of α + β microstructures produced by these TPs present a daunting challenge for both experimental characterization and computer simulation[45] of microstructural evolution during alloy processing and in service, which is critical for microstructure design and optimization. It has been difficult to produce fine α + β microstructures in Ti-alloy components following the conventional transformation pathways. However, it has been recently demonstrated that the Integrated Computational Materials Engineering (ICME) approach[46] has the potential to accelerate the realization of new alloy design ideas by taking full advantage of the complicated TPs present, and optimization of processing conditions for precise control of the TPs in the development of the next generation of Ti-alloys.[47]

Figure 4 shows examples of ultrafine and uniform α + β microstructures with little microtexture, designed by utilizing the pseudospinodal decomposition mechanism[39] for the refined α (Figure 4a)[48] and precursory ω-assisted α precipitation[49,50] for the more-refined and super-refined α (Figure 4b–c). The composition and temperature windows for the pseudospinodal decomposition mechanism to operate, and the effects of compositional (e.g., solute partitioning) and mechanical (e.g., coherency stress field) associated with precipitation and dissolution of isothermal ω particles, are quantified by computer simulations.[39,50] Based on the detailed quantitative understanding developed in these simulations studies, specific alloy compositions and heat treatments can be designed to achieve these ultrafine and microtexture-free α precipitate microstructures at different length scales.

Conclusions

Significant progress has been made on microstructural design for advanced light alloys. This achievement is made by the application of advanced characterization and computation.

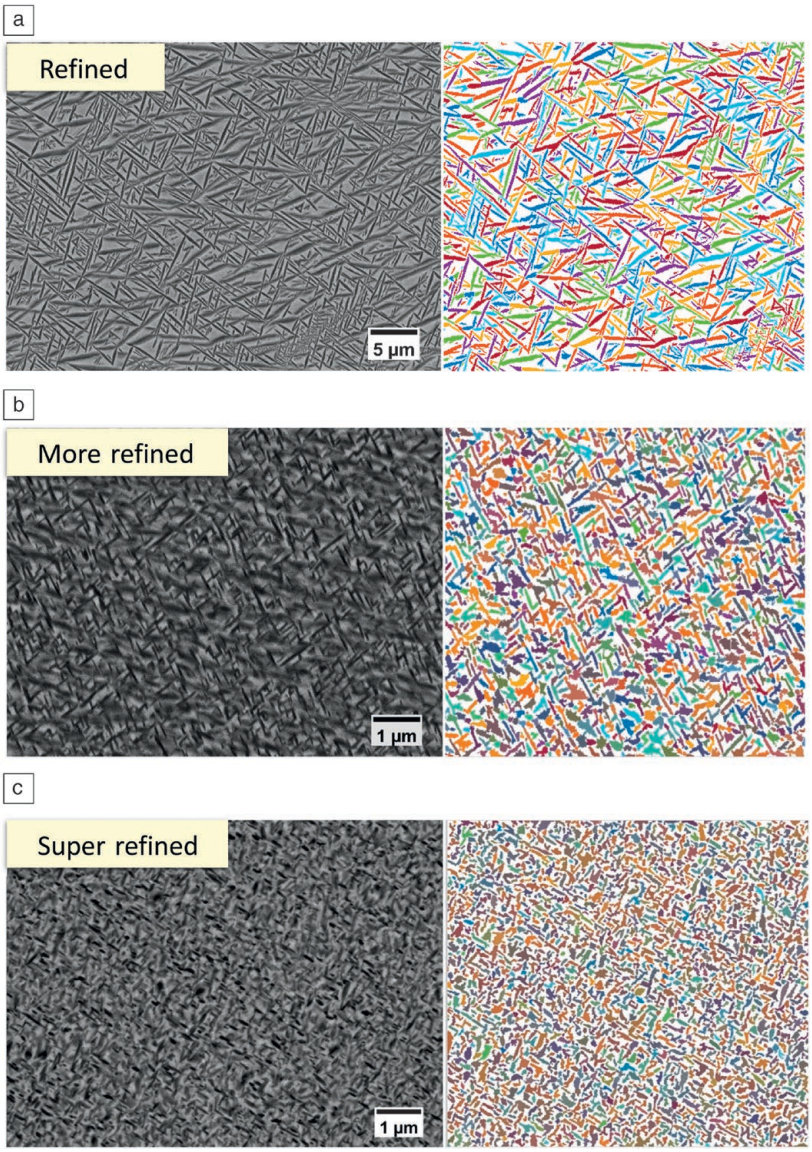


Figure 4. Various scales of ultrafine α + β microstructures. (a) Refined α + β (~5 ppts/μm^2) via pseudospinodal mechanism, where ppts is precipitates;[48] (b) more-refined α + β (~20 ppts/μm^2) via indirect ω-assisted α nucleation;[49] (c) super-refined α + β (~40 ppts/μm^2) via direct ω-assisted α nucleation.[50] The colors (randomly picked) in MIPAR (http://www.mipar.us)-processed images (on the right) represent different α precipitates.

https://doi.org/10.1557/mrs.2019.73 Published online by Cambridge University Press

With the advent of atomic-scale elemental mapping and computation tools for alloys having multiple alloying elements, it is expected that many uncharted territories in alloy microstructure design space will be effectively explored.

Acknowledgments

J.F.N. is grateful to the support of the Australian Research Council. Y.W. acknowledges support from US National Science Foundation under DMREF program Grant No. DMR-1435483. The authors thank Y.F. Zheng for his help in preparing Figure 4.

References

1. H.I. Aaronson, M. Enomoto, J.K. Lee, *Mechanisms of Diffusional Phase Transformations in Metals and Alloys* (CRC Press, Taylor & Francis Group, Boca Raton, FL, 2010).
2. L. Bourgeois, C. Dwyer, M. Weyland, J.F. Nie, B.C. Muddle, *Acta Mater.* **59**, 7043 (2011).
3. K. Hono, N. Sano, S.S. Babu, R. Okano, T. Sakurai, *Acta Metall. Mater.* **41**, 829 (1993).
4. L. Reich, M. Murayama, K. Hono, *Acta Mater.* **46**, 6053 (1998).
5. S.J. Kang, Y.W. Kim, M. Kim, J.M. Zuo, *Acta Mater.* **81**, 501 (2014).
6. M. Murayama, K. Hono, *Scripta Mater.* **44**, 701 (2001).
7. V. Araullo-Peters, B. Gault, F. de Geuser, A. Deschamps, J.M. Cairney, *Acta Mater.* **66**, 199 (2014).
8. S.J. Kang, T.H. Kim, C.W. Yang, J.I. Lee, E.S. Park, T.W. Noh, M. Kim, *Scripta Mater.* **109**, 68 (2015).
9. E. Gumbmann, W. Lefebvre, F. de Geuser, C. Sigli, A. Deschamps, *Acta Mater.* **115**, 104 (2016).
10. H. Liu, Y. Gao, L. Qi, Y. Wang, J.F. Nie, *Metall. Mater. Trans.* **46A**, 3287 (2015).
11. E. Hornbogen, E.A. Starke, *Acta Metall. Mater.* **41**, 1 (1993).
12. J.F. Nie, B.C. Muddle, *J. Phase Equilib.* **19**, 543 (1998).
13. J.F. Nie, B.C. Muddle, *Mater. Sci. Eng. A* **319**, 448 (2001).
14. J.F. Nie, B.C. Muddle, *Acta Mater.* **56**, 3490 (2008).
15. J.F. Nie, N. Wilson, Y.M. Zhu, Z. Xu, *Acta Mater.* **106**, 260 (2016).
16. J.F. Nie, in *Physical Metallurgy*, 5th ed., D.E. Laughlin, K. Hono, Eds. (Elsevier, Amsterdam, The Netherlands, 2014), p. 2009.
17. J.W. Christian, *Prog. Mater. Sci.* **42**, 101 (1997).
18. T.T. Sasaki, K. Oh-ishi, T. Ohkubo, K. Hono, *Scripta Mater.* **55**, 251 (2006).
19. C.L. Mendis, C.J. Bettles, M.A. Gibson, C. Hutchinson, *Mater. Sci. Eng. A* **435**, 163 (2006).
20. C.Q. Liu, H.W. Chen, J.F. Nie, *Scripta Mater.* **123**, 5 (2016).
21. J. Wang, J.P. Hirth, C.N. Tome, *Acta Mater.* **57**, 5521 (2009).
22. X.Z. Liao, J. Wang, J.F. Nie, Y.Y. Jiang, P.D. Wu, *MRS Bull.* **41**, 314 (2016).
23. M.A. Kumar, I.J. Beyerlein, C.N. Tome, *Acta Mater.* **116**, 143 (2016).
24. H. Liu, F.X. Lin, P.Y. Zhao, N. Moelans, Y. Wang, J.F. Nie, *Acta Mater.* **153**, 86 (2018).
25. Y.M. Zhu, S.W. Xu, J.F. Nie, *Acta Mater.* **143**, 1 (2018).
26. Y.M. Zhu, M.Z. Bian, J.F. Nie, *Acta Mater.* **127**, 505 (2017).
27. J.P. Hadorn, K. Hantzsche, S.B. Yi, J. Bohlen, D. Letzig, J.A. Wollmershauser, S.R. Agnew, *Metall. Mater. Trans.* **43A**, 1347 (2012).
28. M. Bugnet, A. Kula, M. Niewczas, G.A. Botton, *Acta Mater.* **79**, 66 (2014).
29. J.P. Hadorn, T.T. Sasaki, T. Nakata, T. Ohkubo, S. Kamado, K. Hono, *Scripta Mater.* **93**, 28 (2014).
30. J.D. Robson, *Metall. Mater. Trans.* **45A**, 3205 (2014).
31. Z.R. Zeng, Y.M. Zhu, S.W. Xu, M.Z. Bian, C.H.J. Davies, N. Birbilis, J.F. Nie, *Acta Mater.* **105**, 479 (2016).
32. G. Lutjering, J.C. Wiliams, *Titanium*, 2nd ed. (Springer, Berlin, 2007).
33. G.E. Totten, D.S. MacKenzie, *ASM Handbook, Volume 4E: Heat Treating of Nonferrous Alloys* (ASM International, Materials Park, OH, 2016).
34. W.G. Burgers, *Physica* **1**, 561 (1934).
35. Y. Gao, R. Shi, J.F. Nie, S.A. Dregia, Y. Wang, *Acta Mater.* **109**, 353 (2016).
36. D. Qiu, R. Shi, D. Zhang, W. Lu, Y. Wang, *Acta Mater.* **88**, 218 (2015).
37. G. Lutjering, *Mater. Sci. Eng. A* **243**, 32 (1998).
38. S. Banerjee, P. Mukhopadhyay, *Phase Transformations: Examples from Titanium and Zirconium Alloys* (Elsevier Science, Oxford, 2007).
39. A. Boyne, D. Wang, R.P. Shi, Y. Zheng, A. Behera, S. Nag, J.S. Tiley, H.L. Fraser, R. Banerjee, Y. Wang, *Acta Mater.* **64**, 188 (2014).
40. T.W. Heo, D.S. Shin, L.Q. Chen, *Metall. Mater. Trans.* **45A**, 3438 (2014).
41. S.L. Semiatin, K.T. Kinsel, A.L. Pilchak, G.A. Sargent, *Metall. Mater. Trans.* **44A**, 3852 (2013).
42. D. Qiu, R. Shi, P. Zhao, D. Zhang, W. Lv, Y. Wang, *Acta Mater.* **112**, 347 (2016).
43. R. Shi, V. Dixit, H.L. Fraser, Y. Wang, *Acta Mater.* **102**, 197 (2016).
44. R.P. Shi, N. Zhou, S. Niezgoda, Y. Wang, *Acta Mater.* **94**, 224 (2015).
45. R.P. Shi, D. Wang, Y. Wang, in *ASM Handbook, Volume 4E: Heat Treating of Nonferrous Alloys,* G.E. Totten, Ed. (ASM International, Materials Park, OH, 2016), p. 573.
46. *Integrated Computational Materials Engineering* (National Academies Press, Washington, DC, 2008).
47. D. Wang, R.P. Shi, Y.F. Zheng, R. Banerjee, H.L. Fraser, Y. Wang, *JOM* **66**, 1287 (2014).
48. Y.F. Zheng, J.M. Sosa, R.E.A. Williams, Y. Wang, R. Banerjee, H.L. Fraser, *Scripta Mater.* **111**, 81 (2016).
49. Y.F. Zheng, R.E.A. Williams, J.M. Sosa, T. Alam, Y. Wang, R. Banerjee, H.L. Fraser, *Acta Mater.* **103**, 165 (2016).
50. Y.F. Zheng, R.E.A. Williams, D. Wang, R.P. Shi, S. Nag, P. Kami, J.M. Sosa, R. Banerjee, Y. Wang, H.L. Fraser, *Acta Mater.* **103**, 850 (2016). □



Jian-Feng Nie is a professor in the Department of Materials Science and Engineering at Monash University, Australia. He received his PhD degree from Monash University in 1993. His current research interests include physical metallurgy of light alloys, crystallography of solid–solid phase transformations, applications of transmission electron microscopy, and processing–microstructure–property relationships. He has published more than 150 journal papers. He was awarded the Marcus Grossmann Young Authors Award of ASM International in 2006, and AIME Champion Mathewson Medal Award of The Minerals, Metals & Materials Society in 2015. He is an editor of *Metallurgical and Materials Transactions*. Nie can be reached by email at jianfeng.nie@monash.edu.



Yunzhi Wang is a professor in the Department of Materials Science and Engineering at The Ohio State University. He received his BSc degree in 1982 and his MSc degree in 1985 in metallurgy from the Northeastern University of China, and his PhD degree in 1995 in materials science from Rutgers University, The State University of New Jersey. His research interests include modeling and simulation of microstructure evolution during transformation and deformation in structural materials, shape-memory alloys, and metallic glasses. He has published more than 200 refereed journal articles (with approximately 100 in *Acta Materialia*). His awards include a National Science Foundation CAREER Award in 1997 and the Fraunhofer Bessel Research Award in 2012 from the Alexander von Humboldt Foundation, Germany. Wang can be reached by email at wang.363@osu.edu.



https://doi.org/10.1557/mrs.2019.73 Published online by Cambridge University Press